Transactions on Modelling and Simulation vol 5, © 1993 WIT Press, www.witpress.com, ISSN 1743-355X

Numerical and experimental modelling of crack systems in homogeneous and nonhomogeneous solids

F. Ferber, O. Hinz, K.P. Herrmann
Laboratorium für Technische Mechanik, Paderborn University, Pohlweg 47-49, W-4790 Paderborn, Germany

ABSTRACT

An overview about the numerical simulation and experimental modelling of cracks arising in plane disk-like models of two-phase composite structures will be given. Shadow optical and photoelastic data were collected from digitally sharpened caustics and isochromatic fringe patterns by using a digital image analysis system.
The shadow optical method represents an important tool for the experimental determination of stress intensity factors at the tips of quasistatically extending and fast running cracks, respectively. Further, the method of caustics can be used for the investigation of plastic zones around crack tips propagating in elasto-plastic materials, for mixed-mode crack problems and other stress concentration problems in the vicinity of holes and bores as well as for the evaluation of contact problems. The geometry of the caustics is proportional to the stress field gradient and therefore the caustic contour can be taken as a quantity for experimental measurements. Based on the caustics equations measuring algorithms can be formulated in order to determine stress intensity factors from experimentally gained caustics.
The numerical simulation of shadow spots and isochromatic fringe patterns, respectively, is based on the fundamental equations of optics. By using the components of the stress field or the displacement vector field obtained by means of a finite element or an analytical calculation the image points for the generation of the associated shadow spots can be determined.
Stress intensity factors were also obtained by a special shadow optical-grid-method and the multi-point method of caustics and isochromatics, respectively. By utilizing digital image processing and computergraphics techniques, a set of menu-driven software is developed for interactively implemented caustics and fringes processing.

INTRODUCTION

Interface cracks represent elementary failure mechanisms arising especially in the high-fiber concentration range of fibrous composites subjected to mechanical and/or thermal loading. In the scope of an experimental failure analysis of

brittle composites the method of caustics is applied to determine stress intensity factors (SIF) or related quantities at crack tips situated in homogeneous components or at the interfaces of composites.
Thereby, in the past a great deal of effort was focused on the problem of interface cracks. Owing to the importance and complexity of this mixed-mode fracture phenomenon a very large volume of literature was accumulated within the past three decades [1-12].
A comprehensive survey of the state-of-the-art discussing also the oscillatory anomalies of the elastic stress and displacement fields near the tip of an interface crack as well as the establisment of an appropriate crack propagation criterion was given by Piva and Viola [1], Rice [13] and Comninou [14].

DIGITAL IMAGE PROCESSING

Computer vision and computer animation deal with the manipulation and interpretation of pictorial information by computers. Pictures result in many application areas in science and engineering.
This paper presents a new method for crack tip stress analysis based on a combination of two techniques, namely the -classical optical methods of stress analysis and modern digital image analysis.
The experimentally obtained isochromatics as well as the shadow spots are imaged by a CCD video camera and this video signal is digitized into an 8-bit (256-level) light-intensity distribution by the digital video frame store. The digital image is stored as a 512x512 pixel array in the frame-memory. A schematic of the experimental set-up as well as the computer network is shown in Fig. 1-a. A main computer program *VIP* (with the basic programs: *KARL* [15] and *BVI* [16]) has been developed in order to implement the different measurement algorithms and simulation techniques (Fig. 1-b).

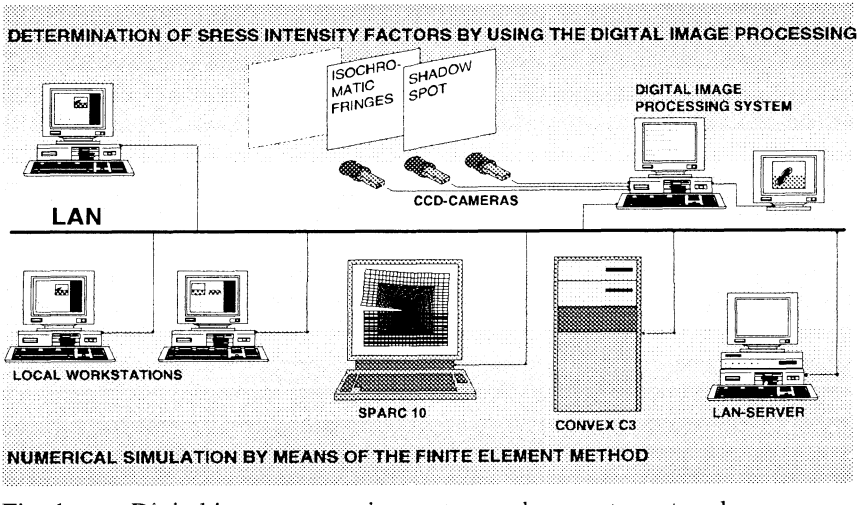

Fig. 1-a. Digital image processing system and computer network

MAIN PROGRAM V I P		
SOFTWARE	KARL	BVI
EXPERIMENT	shadow spots and caustics	isochromatic fringe patterns
THEORY	fracture mechanical parameters	fracture mechanical parameters
	displacement vector field or stress field	stress field
	mapping equation for a shadow spot	basic equations of photoelasticity
	caustic equations	
	measuring algorithm	measuring algorithm
SIMULATION	shadow spots and caustics	isochromatic fringe patterns
DIGITAL IMAGE PROCESSING	measuring algorithm	measuring algorithm
	fracture mechanical parameters	fracture mechanical parameters
SIMULATION	shadow spots and caustics	isochromatic fringe patterns
FINITE ELEMENT METHOD	displacement vector field or stress field	stress field
	fracture mechanical parameters	fracture mechanical parameters
SIMULATION	shadow spots and caustics	isochromatic fringe patterns

Fig. 1-b. Digital image processing system, measurement algorithms and simulation techniques

The numerical simulation of shadow spots and isochromatic fringe patterns, respectively, is based on the fundamental equations of optics. By using the components of the stress field or the displacement vector field of a specimen under plane stress conditions obtained by means of a finite element or an analytical calculation the image points for the generation of the associated shadow spots can be determined.
A summary of some examples is shown in the Figs. 2-3, which contain numerically simulated shadow spots and isochromatic fringe patterns for typical stress concentration problems.

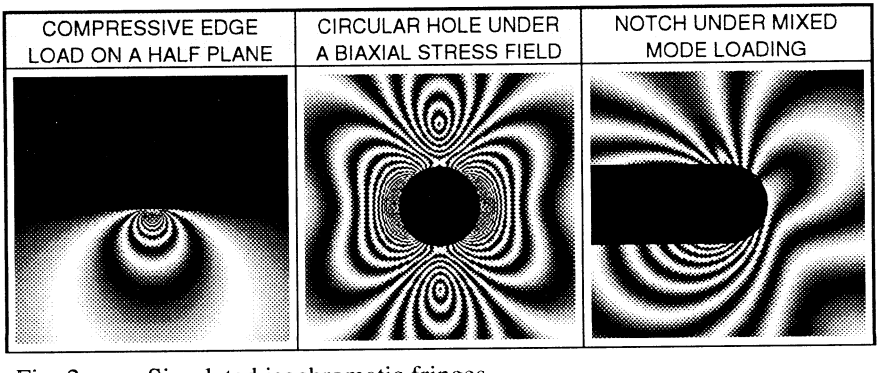

Fig. 2. Simulated isochromatic fringes

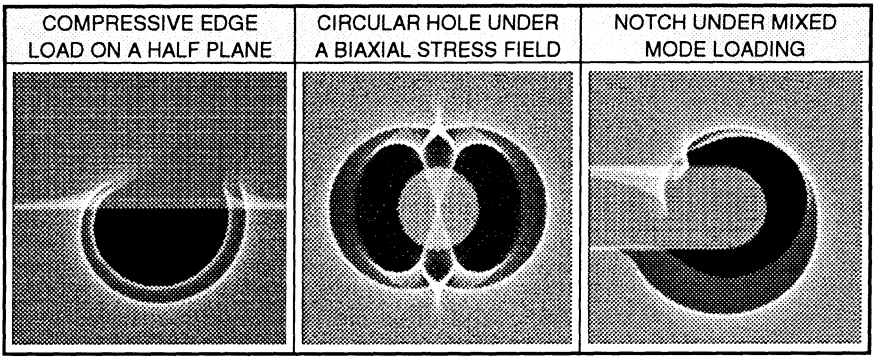

Fig. 3. Simulated shadow spots in the case of optical anisotropy

SIMULATION TECHNIQUES

In this paper, a semi-infinite straight interface crack is considered located in the interface of two half-planes consisting of homogeneous, isotropic and linearly elastic materials with different elastic properties (j = 1,2) (Fig. 4). By introducing the boundary and continuity conditions, respectively, the singular stress field in the vicinity of such an interface crack tip can be expressed in the form

$$\sigma_{lmj} = \frac{e^{\beta(\varphi+\pi(-1)^j)}}{2\cosh(\pi\beta)}\frac{1}{\sqrt{2\pi r}}\left\{K_I f_{lmj}{}^{I}(\varphi) + K_{II} f_{lmj}{}^{II}(\varphi)\right\}; \quad (l,m) = (x,y) \tag{1}$$

$$f_{xxj}{}^{I} = 3\cos(\tfrac{1}{2}\varphi) - \sin\varphi\left(\sin(\tfrac{3}{2}\varphi) - 2\beta\cos(\tfrac{3}{2}\varphi)\right) - e^{-2\beta(\varphi+\pi(-1)^j)}\cos(\tfrac{1}{2}\varphi)$$

$$f_{xxj}{}^{II} = -3\sin(\tfrac{1}{2}\varphi) - \sin\varphi\left(\cos(\tfrac{3}{2}\varphi) + 2\beta\sin(\tfrac{3}{2}\varphi)\right) - e^{-2\beta(\varphi+\pi(-1)^j)}\sin(\tfrac{1}{2}\varphi)$$

$$f_{yyj}{}^{I} = \cos(\tfrac{1}{2}\varphi) + \sin\varphi\left(\sin(\tfrac{3}{2}\varphi) - 2\beta\cos(\tfrac{3}{2}\varphi)\right) + e^{-2\beta(\varphi+\pi(-1)^j)}\cos(\tfrac{1}{2}\varphi)$$

$$f_{yyj}{}^{II} = -\sin(\tfrac{1}{2}\varphi) + \sin\varphi\left(\cos(\tfrac{3}{2}\varphi) + 2\beta\sin(\tfrac{3}{2}\varphi)\right) + e^{-2\beta(\varphi+\pi(-1)^j)}\sin(\tfrac{1}{2}\varphi)$$

$$f_{xyj}{}^{I} = \sin(\tfrac{1}{2}\varphi) + \sin\varphi\left(\cos(\tfrac{3}{2}\varphi) + 2\beta\sin(\tfrac{3}{2}\varphi)\right) - e^{-2\beta(\varphi+\pi(-1)^j)}\sin(\tfrac{1}{2}\varphi)$$

$$f_{xyj}{}^{II} = \cos(\tfrac{1}{2}\varphi) - \sin\varphi\left(\sin(\tfrac{3}{2}\varphi) - 2\beta\cos(\tfrac{3}{2}\varphi)\right) + e^{-2\beta(\varphi+\pi(-1)^j)}\cos(\tfrac{1}{2}\varphi)$$

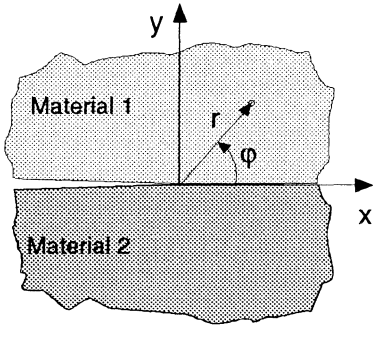

ν_j = Poisson's ratio

G_j = Shear modulus

E_j = Young's modulus

β = Bimaterial constant

$$\beta = \frac{1}{2\pi}\ln\left(\frac{\frac{\kappa_1}{G_1}+\frac{1}{G_2}}{\frac{1}{G_1}+\frac{\kappa_2}{G_2}}\right)$$

$$\kappa_j = \frac{3-\nu_j}{1+\nu_j} \text{ ; (plane stress)}$$

$$\kappa_j = 3-4\nu_j \text{ ; (plane strain)}$$

Fig. 4. Straight interface crack

Simulation of Isochromatic Fringe Patterns

In this part the isochromatic fringe patterns simulation developed in the vicinity of a crack tip lying in the interface of two bonded dissimilar materials are studied.

$$I_j(r,\varphi) = I_{1j} + I_{2j}\sin^2\left(\frac{d_{eff}\pi}{S_j}\left[\sigma_1(r,\varphi) - \sigma_2(r,\varphi)\right]_j\right); \quad S_j = S_c\frac{(1+\nu_c)E_j}{(1+\nu_j)E_c} \qquad (2)$$

I_j = Light intensity
I_{1j} = Reference light intensity
I_{2j} = Reference light intensity
d_{eff} = Effective thickness
ν_c = Poisson's ratio of the coating
E_c = Young's modulus of the coating
S_j = Photoelastic constant
S_c = Photoelastic constant of the coating

By using the stress components, eq. (1), and the light-intensity variations, eq. (2), the isochromatic fringe patterns for different loading conditions were simulated (Fig. 5).

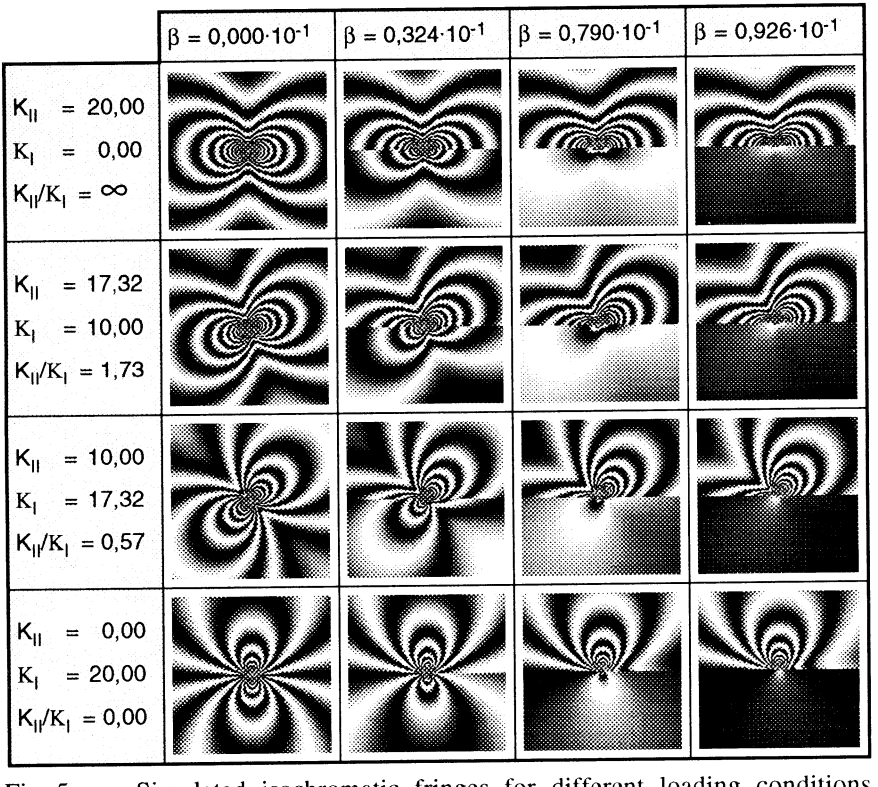

Fig. 5. Simulated isochromatic fringes for different loading conditions around the tip of a straight interface crack

Simulation of Shadow Spots

Figure 6 shows the light deviation induced by the stress field singularity which generates a shadow spot in the reference plane. The bright limit curve of the shadow spot is called caustic. A treatment of cracked opaque model materials can also be performed because the method of caustics can be used in transmission as well as in reflection. Comprehensive reviews about the shadow optical method of caustics were given by Theocaris [8], Kalthoff [9] and Rossmanith [17].

The physical principle underlying the method of shadow patterns is illustrated in Fig. 6. A specimen containing a crack which is loaded by tensile stresses is illuminated with light generated by a point light source. In this case a specimen of a transparent material is considered. The stress intensification in the region surrounding the crack tip leads to a reduction of both the thickness of the specimen and the refractive index of the material. As a consequence, in the transmission case, the light passing through the specimen is deflected outwards. Therefore on an image plane at any distance z_0 behind the specimen a dark shadow spot is formed. The spot is bounded by a bright light concentration, the caustic. For optically isotropic materials a single caustic results, while for optically anisotropic materials a double caustic is obtained. For non-transparent materials the light being reflected from the mirrored surface of the specimen forms qualitatively the same shadow pattern as obtained in transmission, when observed in a virtual image plane positioned behind the specimen.

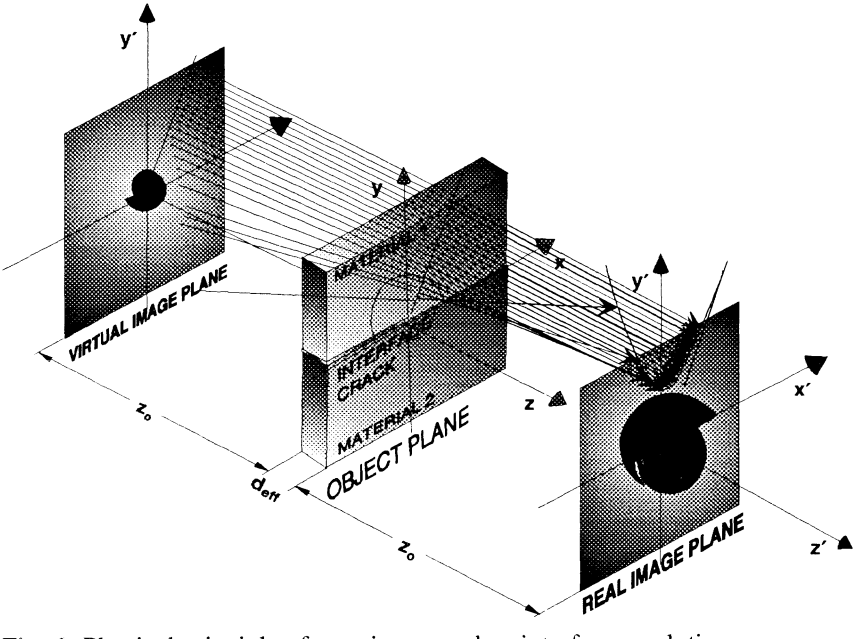

Fig. 6. Physical principle of caustics around an interface crack tip

The light deflections in the reflection case are caused only by the thickness changes of the specimen. Because the magnitude of the light deflections is correlated with the magnitude of the stress intensification at the crack tip, the shadow pattern contains information about the stress-strain conditions in the vicinity of the crack tip and, in particular, about the stress intensity factor. Manogg [18] for the first time calculated the shadow pattern and found quantitative correlations between the dimensions of the caustic and the stress intensity factor. By using Muskhelishvili's complex potentials method as well as by applying the method of conformal mapping a Hilbert-problem for a curvilinear interface crack located in the discontinuity area between two loaded half-planes with different elastic material properties has been solved. This solution allows the derivation of a closed form expression for the total energy release rate G at the crack tip as well as the calculation of strain energy release rates G_i (i = I,II) related to each of the two sides of the material interface [19]. Besides, the generating equations of the mixed mode caustics at the tip of an interface crack have been obtained by means of the complex potentials representing the solution of the associated Hilbert-problem. The general mapping equation for a shadow spot generated in an image plane by convergent light penetrating a transparent two-phase composite structure containing an interface crack reads as follows

$$w_j = m\left\{r_j - C_j\left[\nabla\left(\sigma_1+\sigma_2\right)_j \pm \lambda_j \nabla\left(\sigma_1-\sigma_2\right)_j\right]\right\};\quad (j=1,2) \tag{3}$$

with the definition of the mapping scale m = z2/(zo + z2) of the experimental set-up and the corresponding constants C_j for transmitted and reflected light, respectively

$$C_j = \frac{z_0 d_{eff} c_j}{m} \text{ for transmission};\qquad C_j = \frac{z_0 d_{eff} \nu_j}{m E_j} \text{ for reflection} \tag{4}$$

where z_o and z_2 are special distances of the experimental set-up, d_{eff} is the thickness of the specimen and c_j and λ_j are the shadow optical constants and the so-called optical anisotropy constants, respectively. The caustic can be obtained by introducing the so-called initial curve r = r(φ) into eq. (3). By considering the specialization m=1 as well as optical isotropy of the compound the following equations for the caustics around the crack tip are obtained [20]

$$w_j = r_j\left\{e^{i\varphi} + \frac{R_1 R_2}{R_3} e^{i\left[\beta\left(\ln R_1 + \ln r_j\right) + \frac{3}{2}\left(\varphi-\gamma_1\right)+\gamma_2-\eta+\omega\right]}\right\} \tag{5}$$

with the definition of the initial curves of the caustics

$$r_j = \frac{1}{R_1}\left\{\left(K_{I_j}^2 + K_{II_j}^2\right)\left(1+4\beta^2\right)\right\}^{\frac{1}{5}}\left(2C_j R_3\right)^{\frac{2}{5}} e^{\frac{2}{5}\beta\left(\varphi-\gamma_1\right)} \tag{6}$$

where the radii R_1, R_2, R_3, and angles γ_1, γ_2 are correcting functions.

A summary of some examples is shown in Fig. 7, which contains numerically simulated caustics for straight interface cracks situated in the discontinuity area of a two-phase compound. Thereby the caustics were obtained by an evaluation of eqs. (1) for a material combination of Epoxy (Material 1) / Modified Epoxy (Material 2).

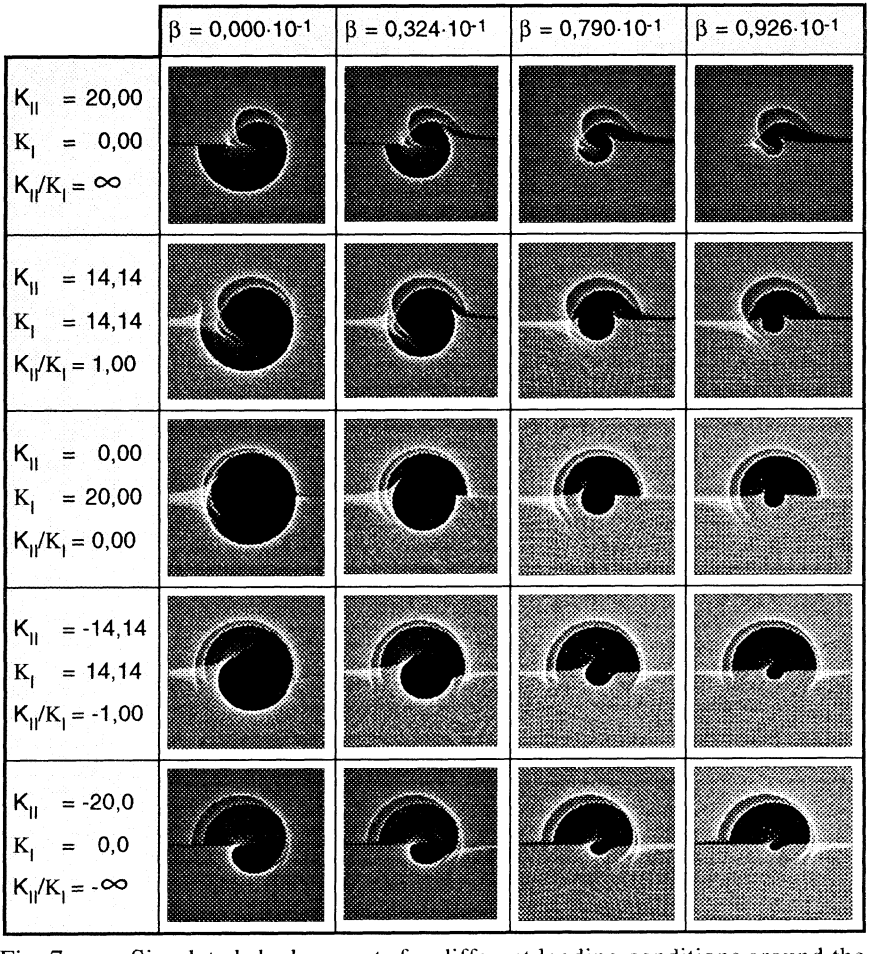

Fig. 7. Simulated shadow spots for different loading conditions around the tip of a straight interface crack

Numerical Simulation by Means of the Finite Element Method

By using the components of the stress field of a specimen under plane stress conditions obtained by means of a finite element calculation the isochromatic fringe patterns can be determined. Figure 8 shows the finite element meshes for a CT-specimen under constant external load containing a straight matrix crack.

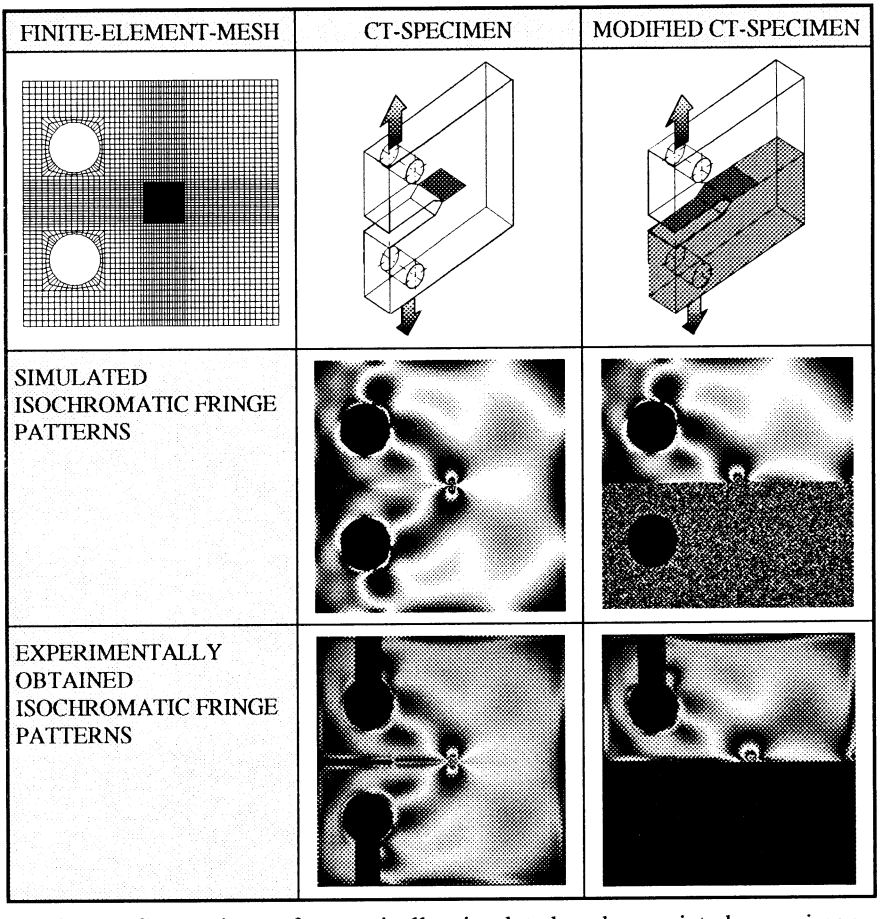

Fig. 8. Comparison of numerically simulated and associated experimentally obtained isochromatic fringe patterns for a standard as well as for a modified version of a CT-specimen

The numerical simulation of the shadow spots by means of the finite element method can be based on the fundamental equation of the shadow optical method in reflection for the description of the image points [21].
By consideration of small deformations as well as by performing of several lengthy transformations by using Lame-Navier's equations for a plane stress state under neglecting of volume forces the fundamental equation of the shadow optical method can be reformulated.

$$X_i = x_i - 2\{z_0 - f(x_i)\}\frac{grad\, f(x_i)}{1-|grad\, f(x_i)|^2}\ ; \quad (i=1,2) \tag{7}$$

Further, these equations read in case of small deformations

$$X_i = x_i - 2z_0 grad\, f(x_i)\ ; \ (i=1,2) \tag{8}$$

By using the relationships

$$f(x_i) = -u_3(x_i) \; ; \; u_3(x_i) = \frac{d_{eff}}{2} \varepsilon_{33}(x_i) \tag{9}$$

the equations (8) can be reformulated into the following relations

$$X_i = x_i + z_0 d_{eff} \, grad \, \varepsilon_{33}(x_i) \tag{10}$$

Moreover, by using Lame-Navier's equations for a plane stress state

$$\mu \Delta u_i + \left\{ \frac{2\lambda\mu}{\lambda + 2\mu} + \mu \right\} e_{,i} = 0 \tag{11}$$

with the definitions of Lame's constants

$$\lambda = \frac{E\nu}{(1+\nu)(1-2\nu)} \; ; \quad \mu = \frac{E}{2(1+\nu)} \tag{12}$$

and under consideration of the following relations

$$e = \varepsilon_{11} + \varepsilon_{22} \; ; \quad \varepsilon_{33} = -\frac{\nu}{1-\nu}(\varepsilon_{11} + \varepsilon_{22}) \tag{13}$$

the equations (8) can be reformulated into

$$X_i = x_i + \frac{z_0 d_{eff} \nu}{1+\nu} \Delta u_i \tag{14}$$

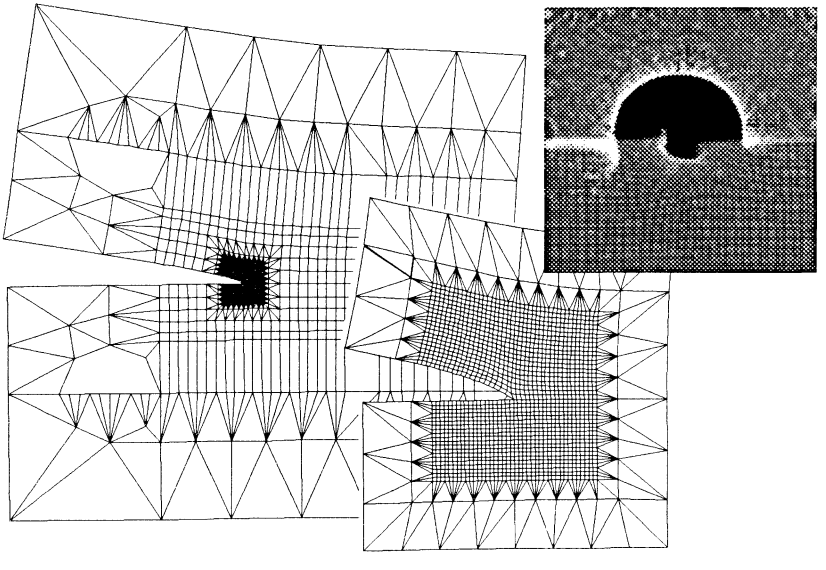

Fig. 9. Finite element mesh with "window" and numerically simulated shadow spots in a modified CT-specimen

Thus, by using the components of the displacement vector field of a specimen under plane stress conditions obtained by means of a finite element calculation

the image points for the generation of the associated shadow spots can be determined [12].

Figure 9 shows the finite element meshes for a Compact Tension specimen under constant external load containing a straight matrix crack. Thereby the given total finite element mesh consists of several substructures which can be either generated by means of special programs or implemented by hand through the user.
A confirmation of the results is shown in Fig. 9 which contains numerically simulated caustics for a straight interface crack.

DETERMINATION OF STRESS INTENSITY FACTORS BY USING THE DIGITAL IMAGE PROCESSING

More and more of the great potential of modern digital image-analysis systems is being uncovered through optical test procedures such as photoelasticity, holography, Moire- technique, speckle photography and the method of caustics, respectively.

Shadow-Optical-Grid Method

By applying the general mapping equations for a mixed-mode shadow spot

$$x' = m\left[r\cos\varphi + z_0 c d_{eff} \sqrt{\frac{K_I^2 + K_{II}^2}{2\pi r^3}} \cos\left(\frac{3}{2}\varphi + \omega\right)\right] \tag{15}$$

$$y' = m\left[r\sin\varphi + z_0 c d_{eff} \sqrt{\frac{K_I^2 + K_{II}^2}{2\pi r^3}} \sin\left(\frac{3}{2}\varphi + \omega\right)\right]$$

the determination of stress intensity factors K_I and K_{II} by using a digital image analysis system is possible. By using the definitions

$$\mu = \frac{K_I}{K_{II}} = \frac{(y'-y) - (x'-x)\tan\left(\frac{3}{2}\varphi\right)}{(x'-x) + (y'-y)\tan\left(\frac{3}{2}\varphi\right)} \; ; \quad \mu = \tan(\omega) \tag{16}$$

with

$$K_I = \frac{1}{z_0 c d_{eff}} \sqrt{\frac{2\pi r^3 \left\{(y'-y)^2 + (x'-x)^2\right\}}{1+\mu^2}} \; ; \quad K_{II} = \mu K_I \tag{17}$$

and the measuring points P(x,y) and P'(x',y') an application of an image processing is possible in order to measure the coordinates of the points P (grid point) and P' (corresponding deformed point). A representative example of the shadow-optical-grid method is shown in Fig. 10. This method is especially useful for the determination of stress intensity factors K_I and K_{II} in the case of a virtual pattern.

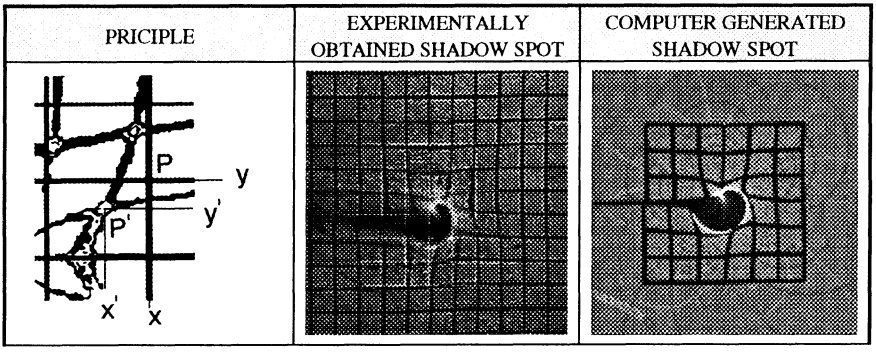

Fig. 10. Shadow-optical-grid method

Characteristic Length Method

The well known caustics equations can be formulated in a modified version because by using the two distances X_x and Y_y defined in Fig. 11, the two stress intensity factors K_I and K_{II} can be determined as follows:

$$K_I = \frac{2C}{3}\sqrt{\frac{2\pi}{m^3}}\left\{\left(\frac{X_x}{f_x}\right)^2 + \left(\frac{Y_y}{f_y}\right)^2\right\}^{\frac{5}{4}} \cos(\omega) \tag{18}$$

$$K_{II} = \frac{2C}{3}\sqrt{\frac{2\pi}{m^3}}\left\{\left(\frac{X_x}{f_x}\right)^2 + \left(\frac{Y_y}{f_y}\right)^2\right\}^{\frac{5}{4}} \sin(\omega)$$

with the definition

$$\omega = \frac{5}{2}\arctan\frac{X_x f_y}{Y_y f_x}$$

$f_x = 1{,}9593$ numerical factor

$f_y = 3{,}1702$ numerical factor

$C = z_0 d_{eff} c$ transmission case

$C = z_0 d_{eff} \frac{\nu}{E}$ reflection case

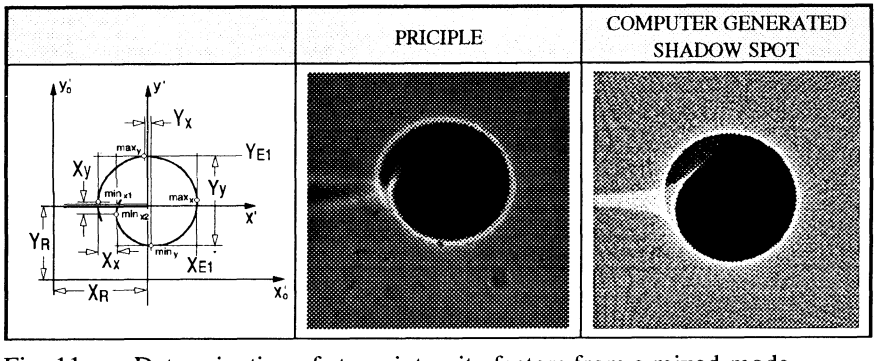

Fig. 11. Determination of stress intensity factors from a mixed-mode caustic

Figure 11 obtains the results of the evaluation of equation (18). Thereby the graph shows an experimentally gained mixed-mode caustic around the tip of a straight matrix crack in the case of optical isotropy of the material.
The position of the crack tip obtainable from an associated experimentally gained shadow spot is given by the following formula.

$$X_R = X_{E1} - \left[\frac{3}{2}C\sqrt{\frac{\left(K_I^2 + K_{II}^2\right)m^3}{2\pi}}\right]^{\frac{2}{5}}\left[\frac{5}{3}\cos\left(\frac{2}{5}\omega\right)\right] \tag{19}$$

$$Y_R = Y_{E1} - \left[\frac{3}{2}C\sqrt{\frac{\left(K_I^2 + K_{II}^2\right)m^3}{2\pi}}\right]^{\frac{2}{5}}\left[\sin\left(\frac{2}{5}(\pi-\omega)\right)+\frac{2}{3}\sin\left(\frac{2}{5}(\pi-\omega)\right)\right]$$

Multiple-Point Method of Photoelasticity

A method for a more accurate determination of stress intensity factors from isochromatic fringe patterns by using numerous appropriate measuring points has been provided for the first time by Sanford and Dally [10]. By using the stress components near a straight interface crack tip as well as the basic equation of the photoelasticity the function g_k for a photoelastic data point k can be expressed as follows

$$g_k(K_I, K_{II}, a_3, \ldots, a_N) = \left(\frac{\sigma_{rr}(r_k,\varphi_k)_j - \sigma_{\varphi\varphi}(r_k,\varphi_k)_j}{2}\right)^2 + \tau_{r\varphi}^2(r_k,\varphi_k)_j - \left(\frac{S_j n_k}{2d_{eff}}\right)^2 = 0 \tag{20}$$

After taking a Tailor's series expansion of g_k and retaining only the linear terms a system of algebraic equations can be obtained

$$g_{k_{i+1}} = g_{k_i} + \left(\frac{\partial g_k}{\partial K_I}\right)_i \Delta K_I + \left(\frac{\partial g_k}{\partial K_{II}}\right)_i \Delta K_{II} + \left(\frac{\partial g_k}{\partial a_3}\right)_i \Delta a_3 + \ldots + \left(\frac{\partial g_k}{\partial a_N}\right)_i \Delta a_N \tag{21}$$

where i refers to the ith iteration step.
A standard Newton-Raphson procedure can be used to calculate the stress intensity factors K_I and K_{II} for a set of proper input data points (Fig. 12).
By utilizing digital-image-processing and computergraphics techniques, a set of menu-driven software has been developed for interactively implemented fringes processing.

Material 1: Araldite B	Material 2: ABS	Geometry:
$E_1 = 3{,}50 \cdot 10^3$ Nmm^{-2}	$E_2 = 3{,}00 \cdot 10^3$ Nmm^{-2}	$d_{eff} = 5{,}00$ mm
$\nu_1 = 0{,}37$	$\nu_2 = 0{,}35$	$x_w = 21{,}00$ mm
$S_1 = 10{,}90$ Nmm^{-1} fr^{-1}	$S_2 = \infty$ Nmm^{-1} fr^{-1}	$y_w = 21{,}00$ mm

Experimentally obtained isochromatic fringe pattern	Data points arrangement for digital image analysis	Computer generated isochromatic fringe pattern
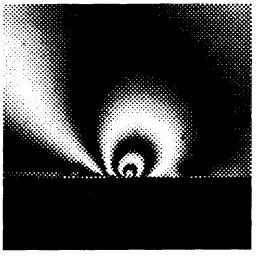	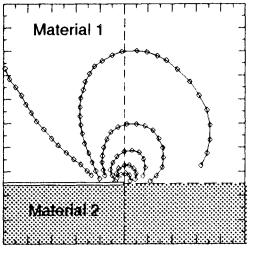	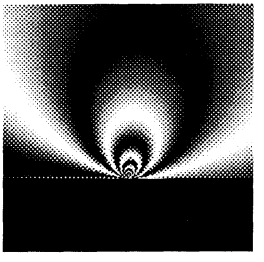

$K_I = 19{,}53$ Nmm$^{-3/2}$; $K_{II} = 1{,}17$ Nmm$^{-3/2}$

Material 1: Araldite B	Material 2: Aluminum	Geometry:
$E_1 = 3{,}50 \cdot 10^3$ Nmm^{-2}	$E_2 = 7{,}22 \cdot 10^4$ Nmm^{-2}	$d_{eff} = 5{,}00$ mm
$\nu_1 = 0{,}37$	$\nu_2 = 0{,}35$	$x_w = 6{,}10$ mm
$S_1 = 10{,}90$ Nmm^{-1} fr^{-1}	$S_2 = \infty$ Nmm^{-1} fr^{-1}	$y_w = 6{,}10$ mm

Experimentally obtained isochromatic fringe pattern	Data points arrangement for digital image analysis	Computer generated isochromatic fringe pattern
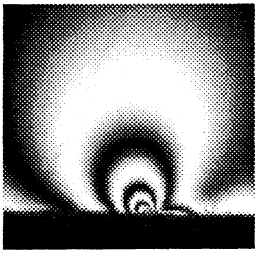	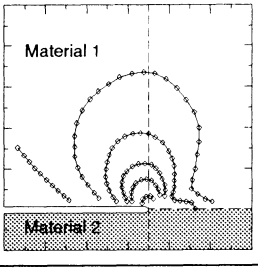	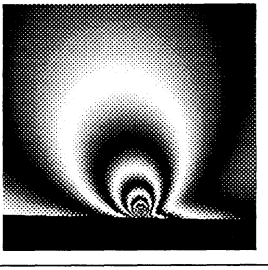

$K_I = 13{,}66$ Nmm$^{-3/2}$; $K_{II} = -2{,}72$ Nmm$^{-3/2}$

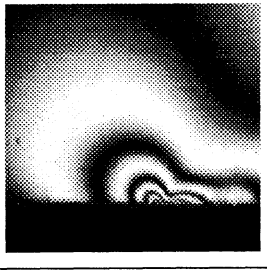

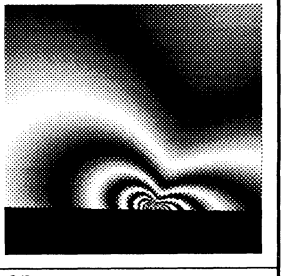

$K_I = 6{,}21$ Nmm$^{-3/2}$; $K_{II} = -8{,}35$ Nmm$^{-3/2}$

Fig. 12.

Fig. 12. Experimental determination of mixed-mode stress intensity factors from an isochromatic fringe pattern around a straight interface crack tip by using the multiple-point method
(Bimaterial constant: Araldite B/ABS $\beta = -0{,}39 \cdot 10^{-2}$)
(Bimaterial constant: Araldite B/Aluminum $\beta = 4{,}06 \cdot 10^{-2}$)

Multiple-Point Method of Caustics

For a more accurate and more complete recording of the caustic geometry the application of a digital image system has been included into the evaluation process, since the latter allows the usage of numerous appropriate measuring points along the caustic contour. The basic idea given by Sanford and Dally can also be applied to the method of caustics. Based on the derived caustics equations a measuring algorithm can be formulated in order to determine stress intensity factors from experimentally gained caustics.

Computer generated shadow spots	Data points arrangement for digital image analysis
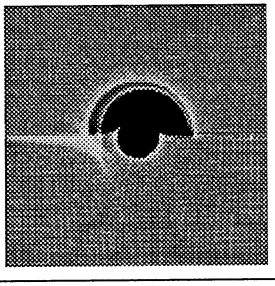	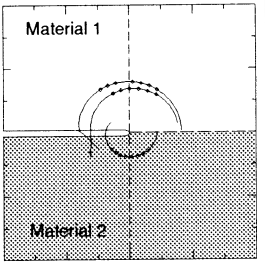
K_I = 10,00 Nmm$^{-3/2}$ K_{II} = 2,00 Nmm$^{-3/2}$	K_I = 9,99 Nmm$^{-3/2}$ K_{II} = 1,99 Nmm$^{-3/2}$

Fig. 13-a.
Shadow spots around a straight interface crack tip in the case of optical anisotropy of the material combination Araldite B and modified epoxy

Numerically simulated shadow spots by means of a finite element calculation	Data points arrangement for digital image analysis
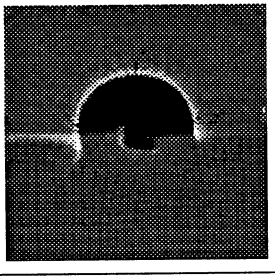	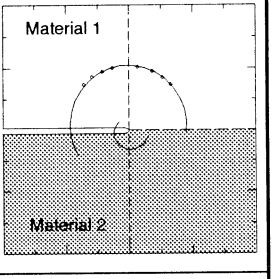
K_I = 29,20 Nmm$^{-3/2}$ K_{II} = -5,70 Nmm$^{-3/2}$	K_I = 30,60 Nmm$^{-3/2}$ K_{II} = -5,20 Nmm$^{-3/2}$

Fig. 13-b.
Shadow spots around a straight interface crack tip of the material combination PMMA and Aluminum in reflection

The caustics equations can be only formulated in an explicit manner if the functional determinant can be solved for the inital curve r= r(φ). This fundamental requirement can only be achieved in the case of a crack in a homogeneous material (β = 0).

Further, it has to be pointed out that in addition to the stress intensity factors K_I and K_{II}, the radii r_k and the angles φ_k, respectively, of the points of the initial curve in the objekt plane are unknown. Moreover, by applying the method of caustics the position of the crack tip can hardly be detected from experimentally gained shadow spots. Thus, the proposed algorithm in [20,22] in which the crack tip position is assumed to be known has been improved.

The new two step algorithm, in the first step, assumes one crack tip coordinate to be known and calculates pairs of stress intensity factors (K_I, K_{II}) depending on the variation of the unknown crack tip coordinate. In the second step, the known and the unknown coordinates are interchanged leading to a second set of stress intensity factors dependig on the other varying crack tip coordinate. The pair of stress intensity factors having the same numerical value represents the required pair of the physical stress intensity factors.

The measuring algorithm has been tested for interface cracks as well as cracks in a homogeneous material in the case of optical anisotropy of the material.

Material 1: PMMA	Material 2: Aluminum	Geometry:
$E_1 = 3{,}24 \cdot 10^3$ Nmm^{-2}	$E_2 = 7{,}22 \cdot 10^4$ Nmm^{-2}	$d_{eff} = 10{,}00$ mm
$\nu_1 = 0{,}35$	$\nu_2 = 0{,}35$	$z_0 = 613{,}00$ mm
$c_1 = 1{,}08\ 10^{-4}$ mm^2 N^{-1}	$c_2 = \infty$ mm^2 N^{-1}	$m = 1{,}00$
Experimentally obtained shadow spot	Data points arrangement for digital image analysis	Computer generated shadow spot
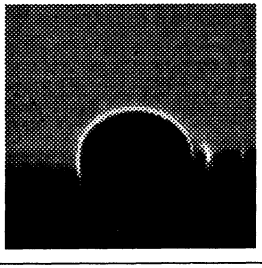	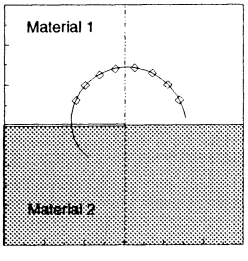	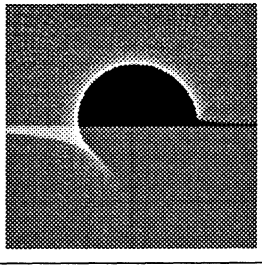
$K_I = 42{,}30$ Nmm$^{-3/2}$; $K_{II} = 22{,}70$ Nmm$^{-3/2}$		

Fig. 14. Experimental determination of mixed-mode stress intensity factors from a shadow spot around a straight interface crack tip by using the multiple-point method (Bimaterial constant: $\beta = 9{,}75 \cdot 10^{-2}$)

The stress intensity factors which have been calculated from a set of measuring points recorded from the caustics in Fig. 13 by using a digital image system have been compared with the stress intensity factors assumed for the associated simulation. The proposed algorithm has provided results for K_I and K_{II} with an

average accuracy of 5 to 10 percent, where each branch of a double caustic has been evaluated separately (Fig. 13-a). The tests have been performed with more than 10 measuring points.
Further, it could be shown that there exists a good agreement between a numerically simulated caustic in transmission for a modified CT-specimen with a straight interface crack and the associated experimental caustic gained by the shadow optical method (Fig. 14).

CONCLUSIONS

A photoelastic interface crack analysis for two-phase compounds has been performed by using the image analysis of isochromatic fringe loops. Morover, the shadow optical method has been applied for the simulation of caustics around the tips of straight interface cracks lying in the discontinuity area of two-phase composite structures. Finally, a computer program for the determination of fracture mechanical parameters like K_I and K_{II}, respectively, was developed by consideration of the so-called multiparameter method. Tests of this software concerning the images obtained experimentally by photoelasticity as well as by the method of caustics demonstrate its usefulness.
Fracture mechanical data like crack surface displacements, strain energy release rates and stress intensity factors have been determined from appropriate finite element calculations. Furthermore, the shadow optical method of caustics has been applied in order to compare the numerically obtained stress intensity factors with the associated experimentally values at which a good coincidence could be stated. The investigations performed by applying the micromechanical method of composite mechanics should lead to a better understanding of the strength and fracture behaviour of composites.

REFERENCES

1. Piva, A. and Viola, E. 'Biaxial Load Effects on a Crack Between Dissimilar Media' *Engineering Fracture Mechanics*, Vol. 13, pp. 143-174, 1980.
2. Irwin, G.R., 'Fracture' *Handbuch der Physik*, ed. S. Flügge, Vol. 6, Springer-Verlag, Berlin/Göttingen/Heidelberg, pp. 551-590, 1958
3. Palaniswamy, K. and Knauss, W.G. 'On the Problem of Crack Extension in Brittle Solids Under General Loading' *Mechanics Today*, Vol. 4, ed. S. Nemat-Nasser, Pergamon Press, New York pp. 87-148, 1978
4. Hayashi, K. and Nemat-Nasser, S. 'Energy-Release Rate and Crack Kinking under Combined Loading' *Journal of Applied Mechanics*, Vol. 48, pp. 521-524, 1981
5. Herrmann, K.P. and Meiners, W. 'On a Generalization of Irwin's Formula Concerning Curvilinear Interface Cracks in Brittle Two-Phase Composite Structures' *Engineering Fracture Mechanics*, Vol. 31, pp. 249-254, 1988 and Vol. 34, pp. 1003, 1989
6. Ferber, F., Ph.D. Dissertation, Paderborn University,1986

7. Ferber, F. and Herrmann, K.P. 'Simulation of Failure Mechanisms in Fibre Reinforced Composites' *VDI-Berichte*, Vol. 731, pp. 303-314, 1989
8. Theocaris, P.S. 'Experimental Evaluation of Stress Concentration and Intensity Factors' *Mechanics of Fracture*, Vol. 7, ed. G.C. Sih, Martinus Nijhoff Publishers, The Hague/ Boston/ London, pp. 189-252, 1981
9. Kalthoff, J.F. 'The shadow optical method of caustics' *Handbook on Experimental Mechanics*, ed. A.S. Kobayashi, Prentice Hall, Englewood Cliffs, pp. 430-500, 1985
10. Sanford, R.J. and Dally, J.W. 'A General Method for Determining Mixed-Mode Stress Intensity Factors from Isochromatic Fringe Patterns' *Engineering Fracture Mechanics*, Vol. 11, pp. 621-633, 1979
11. Ferber, F.; Hinz; O. and Herrmann, K.P. 'Bruchmechanische Analyse von Eigenspannungsproblemen in Verbundgläsern mittels spannungsoptischer Methoden' *VDI-Berichte*, Vol. 815, pp. 459-470, 1990
12. Ferber, F. and Herrmann, K.P. 'Caustics and Fracture Mechanical Quantities at the Tips of Matrix and Curvilinear Interface Cracks Determined by Means of a Finite Element Calculation' *Proceedings of the 9th International Conference on Exp. Mechanics*, Kopenhagen, 20-24 August 1990, ed. V. Askegaard, Aaby Tryk, Kopenhagen, Denmark, Vol. 1, pp. 395-404, 1990
13. Rice, J.R. 'Elastic Fracture Mechanics Concepts for Interfacial Cracks' *Journal of Applied Mechanics*, Vol. 55, pp. 98-103, 1988
14. Comninou, M. 'An Overview of Interface Cracks' *Engineering Fracture Mechanics*, Vol. 55 No. 1, pp. 197-208, 1990
15. Ferber, F., Program Documentation KARL, Paderborn University, 1992
16. Hinz, O., Program Documentation BVI, Paderborn University, 1992
17. Rossmanith, H.P. 'The Caustic Approach to Rayleigh-Waves and their Interaction with Surface Irregularities' *Optics and Lasers in Engineering*, Vol. 14, pp. 115-146, 1991
18. Manogg, P., Ph.D. Dissertation, Freiburg University, 1964
19. Herrmann, K.P. and Noe, A. 'Calculation of Energy Release Rates for Interface Cracks between Dissimilar Linear Elastic Isotropic Materials' *International Journal of Fracture*, Vol. 50, R 51-R58, 1991
20. Herrmann, K.P. and Noe, A. 'Analysis of Quasistatic and Dynamic Interface Crack Extension by the Method of Caustics' *Engineering Fracture Mechanics*, Vol. 42, pp. 573-588, 1992
21. Rosakis, A.J. and Zehnder, A.T. 'On the Method of Caustics: An Exact Analysis Based on Geometrical Optics' *Journal of Elasticity*, Vol. 15, pp. 347-367, 1985
22. Noe, A.; Ferber, F. and Herrmann, K.P. 'Application of the Shadow Optical Method of Caustics for the Analysis of Interface Crack Problems in Composite-Models' *VDI-Berichte*, Vol. 882, pp. 313-324, 1991
23. Ferber, F.; Noe, A.; Hinz, O. and Herrmann, K.P. 'Isochromatics and Caustics around the Tips of Interface Cracks observed by Digital Image Processing' *VDI-Berichte*, Vol. 940, pp. 69-78, 1992